



An efficient cubic spline approximation for variable-order fractional differential equations with time delay

Shole Yaghoobi · Behrouz Parsa Moghaddam · Karim Ivaz

Received: 9 July 2016 / Accepted: 8 September 2016 / Published online: 22 September 2016
© Springer Science+Business Media Dordrecht 2016

Abstract This paper describes a robust, accurate and efficient scheme based on a cubic spline interpolation. The proposed scheme is applied to approximate variable-order fractional integrals and is extended to solve a class of nonlinear variable-order fractional equations with delay. Modified Hutchinson equation and delay Ikeda equation are solved using the proposed scheme. The efficiency and accuracy of the proposed method are analyzed in the perspective of the mean absolute error and experimental convergence order. Numerical results confirm the accuracy and efficiency of the proposed scheme.

Keywords Fractional calculus · Variable-order derivative · Spline approximation · Functional differential equations · Oscillatory dynamic systems

Mathematics Subject Classification 26A33 · 33F05 · 41A15 · 65O15 · 34K37

1 Introduction

Fractional calculus and its applications in many areas in science and engineering have attracted more intention of research communities [1–4]. As given in [5–8] point out, research carried out in recent years shows that the fractional-order differential equations are an effective tool for describing complex dynamics and many physical and engineering systems can be modeled efficiently using them.

Recent decades have witnessed a fast-growing research on developing applications of variable-order (VO) fractional calculus to diverse scientific and engineering fields. More specifically, VO formulations employed to describe the mechanics of an oscillating mass subjected to a variable viscoelasticity damper and a linear spring [9], to characterize the dynamics of van der Pol equation [10] and history of drag expression [11], to analyze elastoplastic indentation problems [12], to interpolate the behavior of systems with multiple fractional terms [13], to develop a statistical mechanics model [14], to obtain variable- order fractional noise [15] and to design new control algorithms [16, 17]. The VO operator definitions recently proposed in the literature include the Riemann–Liouville, Marchaud, Coimbra and Grunwald definitions [9, 13, 18]. There are several set of definitions for the generalized fractional integration operators among which we adopted the one proposed by Leronzo and Hartley [19], VO fractional integration with strong memory of order, stated as

S. Yaghoobi · B. P. Moghaddam (✉)
Department of mathematics, Lahijan Branch, Islamic Azad University, Lahijan, Iran
e-mail: parsa@liau.ac.ir

S. Yaghoobi
e-mail: sholeyaghoobi91@stumail.liau.ac.ir

K. Ivaz
Faculty of Mathematical Sciences, University of Tabriz,
Tabriz, Iran
e-mail: ivaz@tabriz.ac.ir

$$\begin{aligned} {}_{0+}^{V(\cdot)} J_t^{\alpha(t)} y(t) &= \int_{0+}^t \frac{1}{\Gamma(\alpha(t, \tau))} (t - \tau)^{\alpha(t, \tau)-1} y(\tau) d\tau, \\ Re(\alpha(t, \tau)) &> 0. \end{aligned} \quad (1)$$

and VO fractional derivative in the Caputo-base, expressed as follows

$$\begin{aligned} {}_{0+}^{V(\cdot)} D_t^{\alpha(t)} y(t) &= \int_{0+}^t \frac{1}{\Gamma(\kappa - \alpha(t, \tau))} \frac{y^\kappa(\tau) d\tau}{(t - \tau)^{\alpha(t)+1-\kappa}}, \\ \kappa - 1 < \alpha(t) < \kappa. \end{aligned} \quad (2)$$

where $\kappa \in \mathbb{Z}^+$, $y(t)$ is $(\kappa - 1)$ times continuously differentiable, $y^{(\kappa)}(t)$ is once integrable and $\Gamma(\cdot)$ is the gamma function.

There are three main type of VO fractional operators that characterized by changing the form of the argument of $\alpha(t, \tau)$. The following definitions will be considered: $\alpha(t, \tau) = \alpha(t)$, $\alpha(t, \tau) = \alpha(\tau)$, and $\alpha(t, \tau) = \alpha(t - \tau)$.

Definition 1.1 The VO fractional integration type 1 (V1) is given by

$$\begin{aligned} {}_{0+}^{V1} J_t^{\alpha(t)} y(t) &= \frac{1}{\Gamma(\alpha(t))} \int_{0+}^t (t - \tau)^{\alpha(t)-1} y(\tau) d\tau, \\ Re(\alpha(t)) &> 0. \end{aligned} \quad (3)$$

Definition 1.2 The VO fractional integration type 2 (V2) is given by

$$\begin{aligned} {}_{0+}^{V2} J_t^{\alpha(t)} y(t) &= \int_{0+}^t \frac{1}{\Gamma(\alpha(\tau))} (t - \tau)^{\alpha(\tau)-1} y(\tau) d\tau, \\ Re(\alpha(t)) &> 0. \end{aligned} \quad (4)$$

Definition 1.3 The VO fractional integration type 3 (V3) is given by

$$\begin{aligned} {}_{0+}^{V3} J_t^{\alpha(t)} y(t) &= \int_{0+}^t \frac{1}{\Gamma(\alpha(t - \tau))} (t - \tau)^{\alpha(t-\tau)-1} \\ y(\tau) d\tau, \quad Re(\alpha(t)) &> 0. \end{aligned} \quad (5)$$

More details about these operators and their application can be found in [20, 21].

In VO fractional differential equations (VOFDEs), the order of the derivative changes with respect to either the dependent or the independent variables (or both), or parametrically with respect to an external functional behavior [22, 23]. Since the kernel of the VO operators has variable exponent, analytical solutions for the VOFDEs are more difficult to obtain. These naturally lead to rapid increasing developments of numerical methods for VOFDEs [24–27].

The VO fractional delay differential equation (VOFDDE) is a generalization of the fixed-order delay differential equation to arbitrary functional order. Compared to fractional delay differential equations (FDDEs), VOFDDEs have not received much attention, although the potential to characterize complex behavior by the functional order of differentiation or integration is clear, along with necessary background from the application area, in order to motivate our study of VOFDDEs [28–31].

In this paper, we focus our attention on VOFDDEs that formulated by means of VO integration and derivation with $\alpha(t, \tau) = \alpha(\tau)$. The importance of this type of VO derivative was recognized recently, and there is a limited knowledge about its application. Ingman and Suzdalnitsky [32] employed type V2 and attempted to create computational algorithms involving satisfactory agreement between the experimental and theoretical distributions of the numerical data in studies of deformation and vibration of systems made from viscoelastic materials resulted in a variety of concepts and models. In [33], Sun et al. the advantage and potential applications of two VO fractional derivative definitions (types V1 and V2) are highlighted through a comparative analysis of anomalous relaxation process. In this line of thought, in [34], Moghaddam and Machado purpose a stable three-level explicit spline finite difference scheme based on the linear B-spline approximation of the time VO fractional derivative of type V2 and the Du FortFrankel algorithm for a class of nonlinear time variable-order fractional partial differential equations.

Having these ideas in mind, the rest of this paper is organized as follows. In Sect. 2, we design an efficient approach for the VO fractional integral based on cubic spline interpolation. In Sect. 3, two numerical examples are included to illustrate the effectiveness of the numerical approach. In Sect. 4, we extend numerical approach for solving a class of nonlinear VOFDDEs. Moreover, we apply the proposed method to the Hutchinson and Ikeda VOFDDEs. In Sect. 4, we outline the main conclusions.

2 Discretization of the VO fractional integral

Throughout the paper, we always assume $y(t)$ a smooth function defined on $[a, T]$, along with the notations $t_j = a + jh$, $y(t_j) = y_j$, $y'(t_j) = y'_j$, $\alpha(t_j) = \alpha_j$ and $\beta(t_j) = \beta_j$, $j = 0, 1, \dots, [(T - a)/h]$, where h

denotes the uniform step size and $[x]$ takes the integer part of x , being the maximum integer that does not exceed x .

For the time instant t_j , $j = 1, \dots, N - 1$, we need to calculate

$$\begin{aligned} {}_{a+}^{V2} J_t^{\alpha(t)} y(t) &= \int_{a+}^{t_j} \frac{1}{\Gamma(\alpha(\zeta))} (t_j - \zeta)^{\alpha(\zeta)-1} y_j(\zeta) d\zeta, \\ Re(\alpha(t)) &> 0, \end{aligned} \quad (6)$$

where ζ is an auxiliary variable belong to the interval $[a, t_j]$.

We compute the integral by means of a cubic spline $y_j(\zeta)$, with nodes and knots chosen at instants t_k , $k = 0, 1, 2, \dots, j - 1$. The cubic spline $y_j(\zeta)$ is of the form

$$y_j(\zeta) = \sum_{k=0}^j N_{j,k}(\zeta) y_k + \sum_{k=0}^j M_{j,k}(\zeta) y'_{k+1}, \quad (7)$$

where $N_{j,k}(\zeta)$ and $M_{j,k}(\zeta)$ are shape functions and in each interval $[t_k, t_{k+1}]$, for $1 \leq k \leq j - 1$, given by

$$N_{j,k}(\zeta) = \begin{cases} (1 - 2\frac{\zeta - t_k}{t_{k+1} - t_k})(\frac{\zeta - t_{k+1}}{t_{k+1} - t_k})^2, & t_{k-1} \leq \zeta \leq t_k \\ (1 - 2\frac{\zeta - t_{k+1}}{t_{k+1} - t_k})(\frac{\zeta - t_k}{t_{k+1} - t_k})^2, & t_k \leq \zeta \leq t_{k+1} \\ 0, & \text{otherwise} \end{cases}$$

and

$$M_{j,k}(\zeta) = \begin{cases} (\zeta - t_k)(\frac{\zeta - t_{k+1}}{t_{k+1} - t_k})^2, & t_{k-1} \leq \zeta \leq t_k \\ (\zeta - t_{k+1})(\frac{\zeta - t_k}{t_{k+1} - t_k})^2, & t_k \leq \zeta \leq t_{k+1} \\ 0, & \text{otherwise} \end{cases}$$

For $k = 0$ and $k = j$, $N_{j,k}(\zeta)$ is of the form

$$N_{j,0}(\zeta) = \begin{cases} (1 - 2\frac{\zeta - t_0}{t_1 - t_0})(\frac{\zeta - t_0}{t_1 - t_0})^2, & t_0 \leq \zeta \leq t_1 \\ 0, & \text{otherwise} \end{cases}$$

$$a_{j,k} = \begin{cases} -6(2j + 1 + \alpha_0)(-1 + j)^{\alpha_0+2} \\ + j^{\alpha_0}((-6\alpha_0 - 18)j^2 + 12j^3 + \alpha_0^3 + 6\alpha_0^2 + 11\alpha_0 + 6), & k = 0 \\ 6((j - k - 1)^{\alpha_j+2}(2k - 2j - \alpha_k - 1) \\ + (j - k + 1)^{\alpha_j+2}(2k - 2j - \alpha_k + 1 + 4(j - k)^{\alpha_k+3})), & 1 \leq k \leq n - 1 \\ 6(\alpha_j + 1), & k = n \end{cases}, \quad (10)$$

and

$$N_{j,j}(\zeta) = \begin{cases} (1 - 2\frac{\zeta - t_j}{t_j - t_{j+1}})(\frac{\zeta - t_{j+1}}{t_j - t_{j+1}})^2, & t_{j-1} \leq \zeta \leq t_j \\ 0, & \text{otherwise} \end{cases},$$

and for $k = 0$ and $k = j$, $M_{j,k}(\zeta)$ is of the form

$$M_{j,0}(\zeta) = \begin{cases} (\zeta - t_1)(\frac{\zeta - t_0}{t_1 - t_0})^2, & t_0 \leq \zeta \leq t_1 \\ 0, & \text{otherwise} \end{cases},$$

and

$$M_{j,j}(\zeta) = \begin{cases} (\zeta - t_j)(\frac{\zeta - t_{j+1}}{t_j - t_{j+1}})^2, & t_{j-1} \leq \zeta \leq t_j \\ 0, & \text{otherwise} \end{cases}.$$

Therefore, substituting (7) into (6) gives

$$\begin{aligned} {}_{a+}^{V2} J_t^{\alpha(t)} y(t) &\approx \sum_{k=0}^j {}_{a+}^{V2} J_{t_k}^{\alpha_k} y_k \\ &= \sum_{k=0}^j \frac{y_k}{\Gamma(\alpha_k)} \int_{a+}^{t_k} (t_j - \zeta)^{\alpha_k-1} N_{j,k}(\zeta) d\zeta \\ &\quad + \sum_{k=0}^j \frac{y'_k}{\Gamma(\alpha_k)} \int_{a+}^{t_k} (t_j - \zeta)^{\alpha_k-1} \\ &\quad \times M_{j,k}(\zeta) d\zeta \end{aligned} \quad (8)$$

and after some calculations, we obtain

$$\begin{aligned} {}_{a+}^{V2} J_t^{\alpha(t)} y(t) &\approx \sum_{k=0}^j \frac{h^{\alpha_k}}{\Gamma(\alpha_k + 4)} a_{j,k} y_k \\ &\quad + \sum_{k=0}^j \frac{h^{\alpha_k+1}}{\Gamma(\alpha_k + 4)} b_{j,k} y'_k \end{aligned} \quad (9)$$

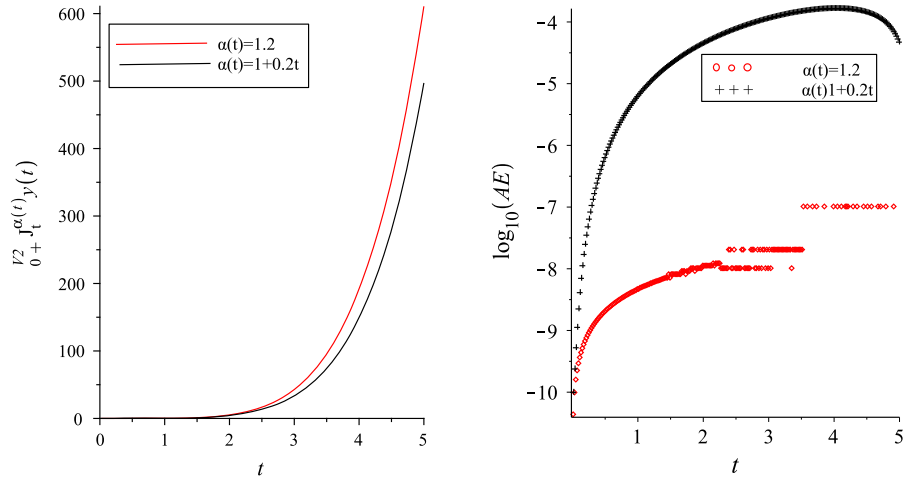
where

$$b_{j,k} = \begin{cases} -(6j + 2\alpha_0)(j - 1)^{\alpha_0+2} + (\alpha_0^2 + (-4j + 5)\alpha_0 + 6(-1 + j))j^{\alpha_0+1}, & k = 0 \\ 2(3k - 3j - \alpha_k)(j - k - 1)^{\alpha_k+2} \\ - 2(3k - 3j + \alpha_k)(j - k + 1)^{\alpha_k+2} - 8(j - k)^{\alpha_k+2}(\alpha_k + 3), & 1 \leq k \leq n - 1 \\ -2\alpha_j, & k = n \end{cases}. \quad (11)$$

and

$$b_{j,k} = \begin{cases} -(6j + 2\alpha_0)(j - 1)^{\alpha_0+2} + (\alpha_0^2 + (-4j + 5)\alpha_0 + 6(-1 + j))j^{\alpha_0+1}, & k = 0 \\ 2(3k - 3j - \alpha_k)(j - k - 1)^{\alpha_k+2} \\ - 2(3k - 3j + \alpha_k)(j - k + 1)^{\alpha_k+2} - 8(j - k)^{\alpha_k+2}(\alpha_k + 3), & 1 \leq k \leq n - 1 \\ -2\alpha_j, & k = n \end{cases}.$$

Fig. 1 The numerical approximation of the VO integral of function $y(t) = t^4$ (left) and magnitude of the $\log_{10}(\text{AE})$ (right), with various values of $\alpha(t)$ and step size $h = 0.01$ in the interval $t \in [0, 5]$



Thus, we get the following discretization formula for the VO fractional integral.

Proposition 2.1 Let $y(t)$ be a function in $C^4[a, T]$ and $\text{Re}(\alpha(t)) > 0$. Then

$$\begin{aligned} {}_{a+}^{V2} J_{t_j}^{\alpha(t)} y(t) &= \sum_{k=0}^j \frac{h^{\alpha_k}}{\Gamma(\alpha_k + 4)} a_{j,k} y_k \\ &\quad + \sum_{k=0}^j \frac{h^{\alpha_k+1}}{\Gamma(\alpha_k + 4)} b_{j,k} y'_k + \mathcal{E}_{V2}(t_j), \end{aligned} \quad (12)$$

where $\mathcal{E}_{V2}(t_j)$ is the approximation error at t_j and is bounded by

$$|\mathcal{E}_{V2}(t_j)| \leq \frac{(t_j - a)^{\alpha^*} |y^{(4)}(t_j)|}{\Gamma(\alpha^* + 1)} O(h^4), \quad (13)$$

where $j = 1, \dots, \left[\frac{(T-a)}{h} \right]$ and

$$\alpha^* = \begin{cases} \sup\{\alpha(t) | \alpha(t) > 0, t \in \mathbb{R}^+\}, & \text{if } t_j \leq 1 \\ \inf\{\alpha(t) | \alpha(t) > 0, t \in \mathbb{R}^+\}, & \text{if } t_j > 1 \end{cases}.$$

3 The numerical method based on cubic spline approximation

In this section, we consider the following initial value problem (IVP) for VOFDDE:

$$\begin{cases} {}_{0+}^{V2} D_t^{\alpha(t)} y(t) = f(t, y(t), y(t-\tau)), & t > 0 \\ y(t) = \phi(t), & -\tau \leq t \leq 0 \end{cases}, \quad (14)$$

where $\kappa - 1 < \alpha(t) \leq \kappa$, τ is the delay time and $\phi(t)$ is the history function defined on the interval $t \in [-\tau, 0]$.

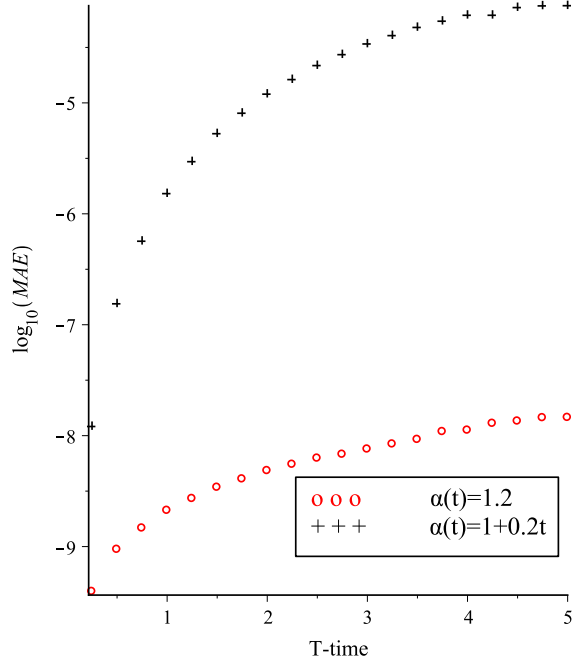


Fig. 2 Magnitude of the $\log_{10}(\text{MAE})$ for approximate VO integral of function $y(t) = t^4$ for various values of $\alpha(t)$ and step size $h = 0.01$ in the interval $t \in [0, T_n = 0.25n]$ where $n = 1, \dots, 20$

The existence and uniqueness of solution for Eq. (14) was investigated by Parsa et al. [35]. This form of nonlinear delayed system is a very general one and includes all well-known delayed systems such as Ikeda system [36], Mackey and Glass system [37], Hopfield delayed neural network [38], delayed Duffing system [39], Delayed Lorenz system [40], BAM neural network [36] and cellular neural network [41].

Fig. 3 The numerical approximation of the VO integral of function $y(t) = t^2 \cos(t)$ (left) and magnitude of the $\log_{10}(\text{AE})$ (right), with various values of $\alpha(t)$ and step size $h = 0.01$ in the interval $t \in [0, 5]$

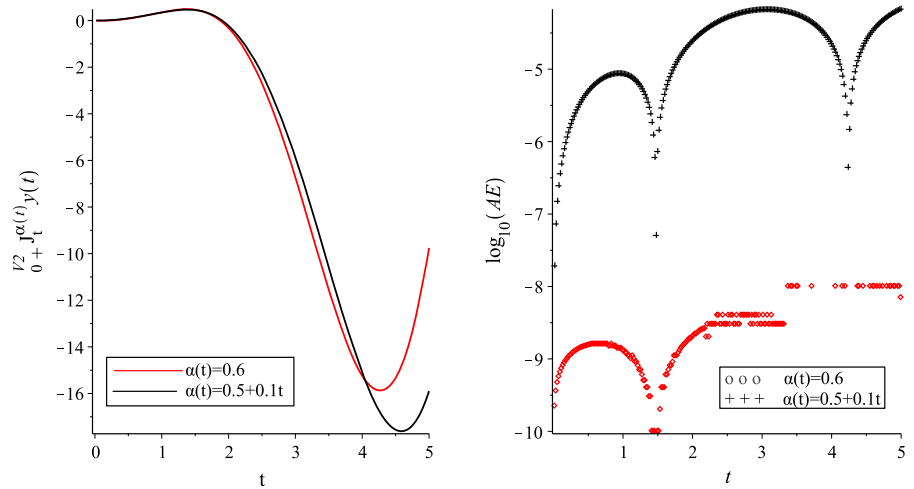


Table 1 Comparison of MAE, ECO and E-time for approximate VO integral of function $y(t) = t^4$ for various values of $\alpha(t)$ and different step sizes in the interval $t \in [0, 5]$

$\alpha(t)$	Step size	MAE	ECO	E-time (s)
$\alpha(t) = 1.2$	$h = \frac{1}{32}$	$1.378211316 \times 10^{-6}$	3.893754293	3.807
	$h = \frac{1}{64}$	$8.263095600 \times 10^{-8}$	3.921457065	16.608
	$h = \frac{1}{128}$	$4.859786778 \times 10^{-9}$	3.945208547	73.773
$\alpha(t) = 1 + 0.2t$	$h = \frac{1}{32}$	$7.943953570 \times 10^{-4}$	2.059571038	11.950
	$h = \frac{1}{64}$	$1.881421686 \times 10^{-4}$	2.062648191	53.399
	$h = \frac{1}{128}$	$4.539303824 \times 10^{-5}$	2.061024204	298.805

Table 2 Comparison of MAE, ECO and E-time for integral VO derivative of function $y(t) = t^2 \cos(t)$ for various values of $\alpha(t)$ and different step sizes in the interval $t \in [0, 5]$

$\alpha(t)$	Step size	MAE	ECO	E-time (s)
$\alpha(t) = 0.6$	$h = \frac{1}{32}$	$2.285069038 \times 10^{-7}$	4.412251781	4.461
	$h = \frac{1}{64}$	$1.472365956 \times 10^{-8}$	4.336214743	18.424
	$h = \frac{1}{128}$	$7.417778124 \times 10^{-10}$	4.332613405	84.521
$\alpha(t) = 0.5 + 0.1t$	$h = \frac{1}{32}$	$1.917652468 \times 10^{-4}$	2.469674218	12.293
	$h = \frac{1}{64}$	$6.052423904 \times 10^{-5}$	2.335354573	57.330
	$h = \frac{1}{128}$	$1.917897719 \times 10^{-5}$	2.238587813	347.883

It is easily noted that Eq. (14) can be transformed to Abel–Volterra integral equation

$$y(t) = T_{k-1}[y; 0](t) + {}_{0+}^{V2}J_t^{\alpha(t)} f(t, y(t), y(t-\tau)), \quad (15)$$

where

$$\begin{aligned} T_{k-1}[y; 0](t) &= \sum_{j=0}^{\kappa-1} \phi^{(j)}(0) \frac{t^j}{j!}, \\ {}_{0+}^{V2}J_t^{\alpha(t)} f(t, y(t), y(t-\tau)) &= \int_{0+}^t \frac{1}{\Gamma(\alpha(\zeta))} (t-\zeta)^{\alpha(\zeta)-1} f(\zeta, y(\zeta), y(\zeta-\tau)) d\zeta. \end{aligned}$$

For solving (15) on $[0, T]$, the interval $[-\tau, T]$ is divided into $m + n$ subintervals, where m and n are integers such that $m = \frac{\tau}{h}$, $n = \frac{T}{h}$ and $t_j = jh$, $j = -m, -m+1, \dots, -1, 0, 1, \dots, n$.

The discretized version of (15) is given as

$$\begin{aligned} y_n &= T_{k-1}[y; 0](t_n) \\ &+ \int_{0+}^{t_n} \frac{1}{\Gamma(\alpha(\zeta))} (t-\zeta)^{\alpha(\zeta)-1} \\ &\times f(\zeta, y(\zeta), y(\zeta-\tau)) d\zeta. \end{aligned} \quad (16)$$

Applying proposed technique in the Sect. 2 to the above equation yields

Table 3 Model 1:
Comparison of MAE, for various values of $\alpha(t)$ and $a = 0.3$, $\tau = 1$, $T = 25$ and different step sizes h

Step size	$\alpha(t) = 1$	$\alpha(t) = 0.8$	$\alpha(t) = 0.04t$
$h = \frac{1}{8}$	$4.711874836 \times 10^{-3}$	$6.857922068 \times 10^{-3}$	$4.476963400 \times 10^{-3}$
$h = \frac{1}{16}$	$2.339301364 \times 10^{-3}$	$3.810693974 \times 10^{-3}$	$2.972195524 \times 10^{-3}$
$h = \frac{1}{32}$	$1.165670474 \times 10^{-3}$	$2.137711972 \times 10^{-3}$	$2.039872992 \times 10^{-3}$

Table 4 Model 1:
Comparison of ECO, for various values of $\alpha(t)$ and $a = 0.3$, $\tau = 1$, $T = 25$ and different step sizes h

Step size	$\alpha(t) = 1$	$\alpha(t) = 0.8$	$\alpha(t) = 0.04t$
$h = \frac{1}{8}$	2.576494357	2.396004258	2.601087920
$h = \frac{1}{16}$	2.184926638	2.008932632	2.098563816
$h = \frac{1}{32}$	1.948924856	1.773943361	1.787460991

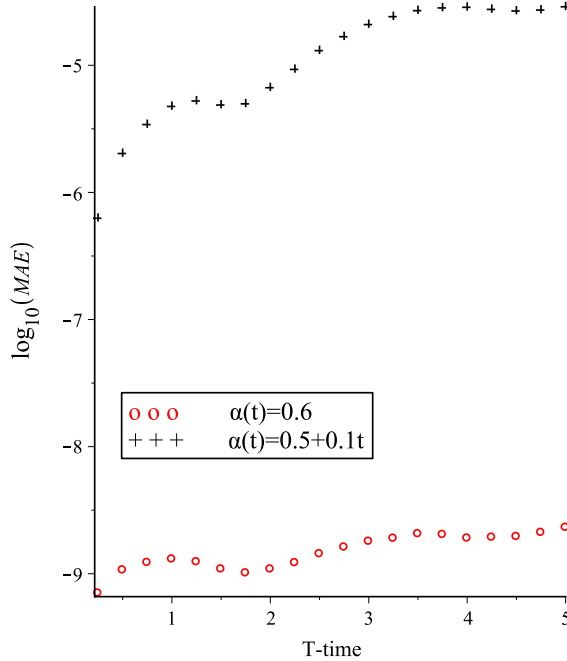


Fig. 4 Magnitude of the $\log_{10}(\text{MAE})$ for approximate VO integral of function $y(t) = t^4$ for various values of $\alpha(t)$ and step size $h = 0.01$ in the interval $t \in [0, T_n = 0.25n]$ where $n = 1, \dots, 20$

$$\begin{aligned} y_n &= T_{\kappa-1}[y; 0](t_n) \\ &+ \sum_{j=0}^n \frac{h^{\alpha_j}}{\Gamma(\alpha_j + 4)} a_{n,j} f(t_j, y_j, y_{j-m}) \\ &+ \sum_{j=0}^n \frac{h^{\alpha_j+1}}{\Gamma(\alpha_j + 4)} b_{n,j} f'(t_j, y_j, y_{j-m}) \end{aligned} \quad (17)$$

where the coefficients $a_{n,j}$ and $b_{n,j}$ are given by (10) and (11), respectively.

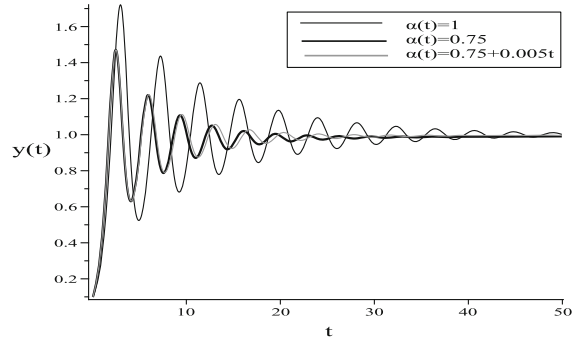


Fig. 5 Time response for Eq. (22), for various values of $\alpha(t)$, with $a = 1.4$, $\tau = 1$ and step size $h = \frac{1}{16}$

For this method, since both side of Eq. (17) include the unknown variable y_n , and due to the nonlinearity of the functions f and f' , it is difficult to derive y_n . Therefore, to achieve a better approximate solution, we substitute a predicted value y_n into the right-hand side of (14).

Let y_n^p be the predicted value, which can be obtained by some simple explicit method. For instance, here we use VO fractional Adams–Bashforth method to drive the predicted value

$$y_n^p = \sum_{j=0}^{\kappa-1} \phi^{(j)}(0) \frac{t_n^j}{j!} + \sum_{j=0}^n c_{j,n} f(t_j, y_j, y_{j-m}), \quad (18)$$

where

$$c_{j,n} = \frac{h^{\alpha_j}}{\Gamma(\alpha_j + 1)} ((n-j)^{\alpha_j} - (n-j-1)^{\alpha_j}), \quad 0 \leq j \leq n.$$

Fig. 6 Time response (left) and phase-space solution (right) for Eq. (22), with $\alpha(t) = 1$, $a = 1.7$, $\tau = 1$ and step size $h = \frac{1}{16}$

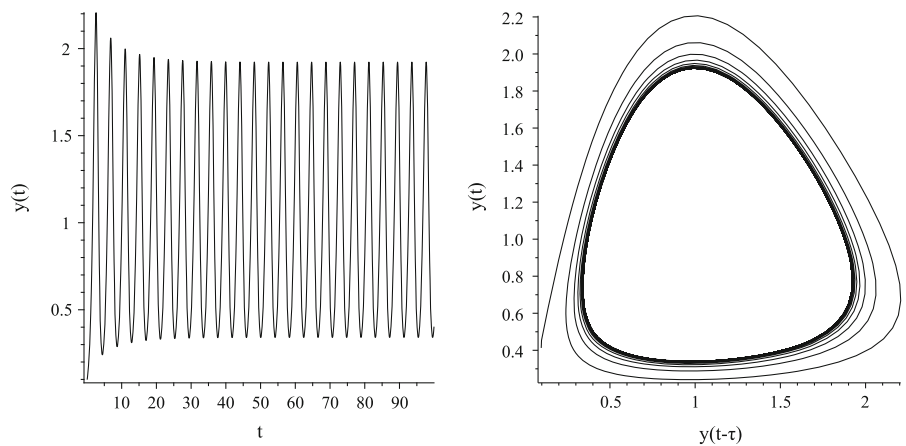


Fig. 7 Time response (left) and phase-space solution (right) for Eq. (22), with $\alpha(t) = 0.7$, $a = 1.7$, $\tau = 1$ and step size $h = \frac{1}{16}$

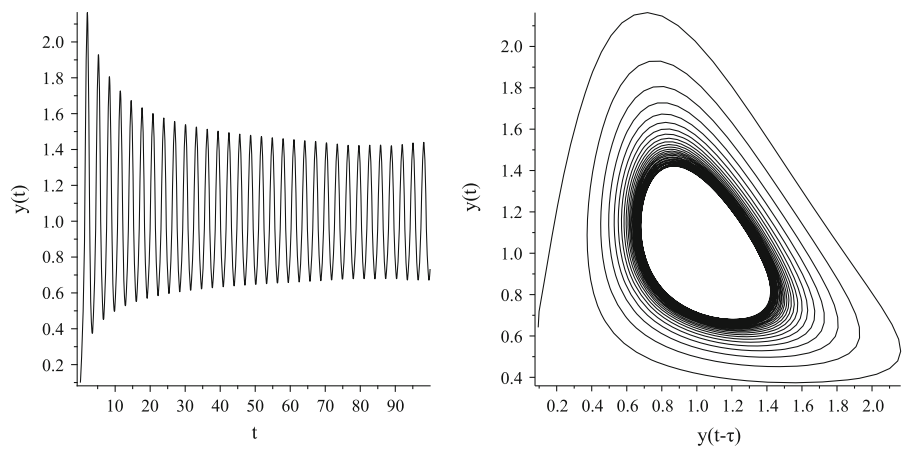


Fig. 8 Time response (left) and phase-space solution (right) for Eq. (22), with $\alpha(t) = 1 - 0.003t$, $a = 1.7$, $\tau = 1$ and step size $h = \frac{1}{16}$

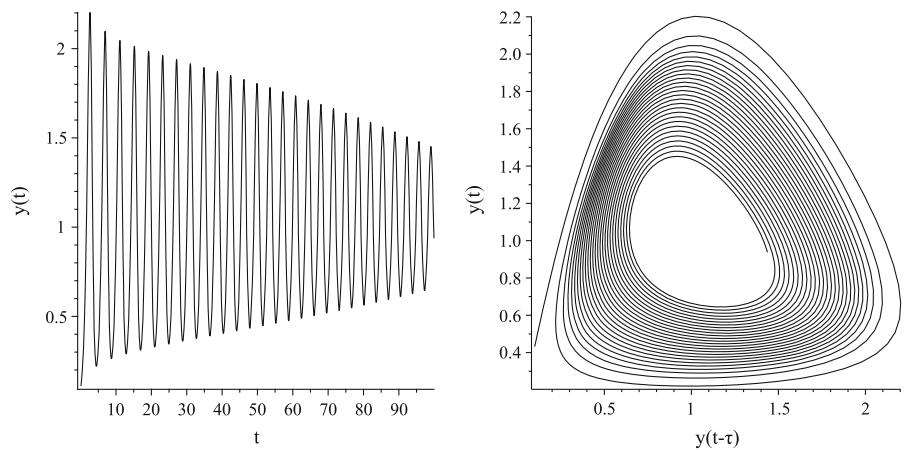


Fig. 9 Time response (left) and phase-space solution (right) for Eq. (23), with $\alpha(t) = 1$, $\lambda = 0$, $\mu = 1$, $\tau = 4$, $\varphi_0 = 2.988$ and step size $h = \frac{1}{16}$

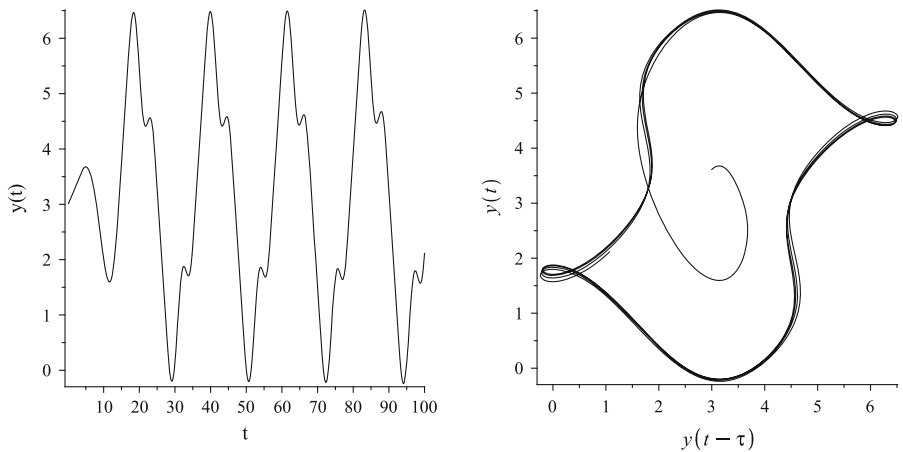


Fig. 10 Time response (left) and phase-space solution (right) for Eq. (23), with $\alpha(t) = 0.75$, $\lambda = 0$, $\mu = 1$, $\tau = 4$, $\varphi_0 = 2.988$ and step size $h = \frac{1}{16}$

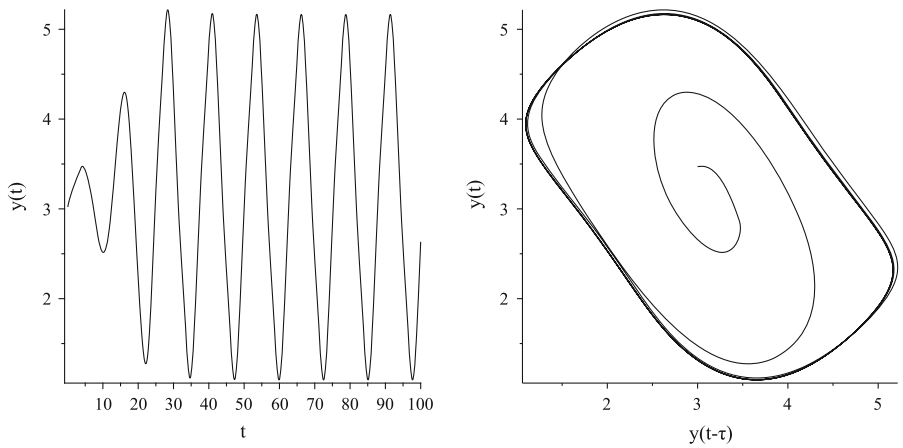
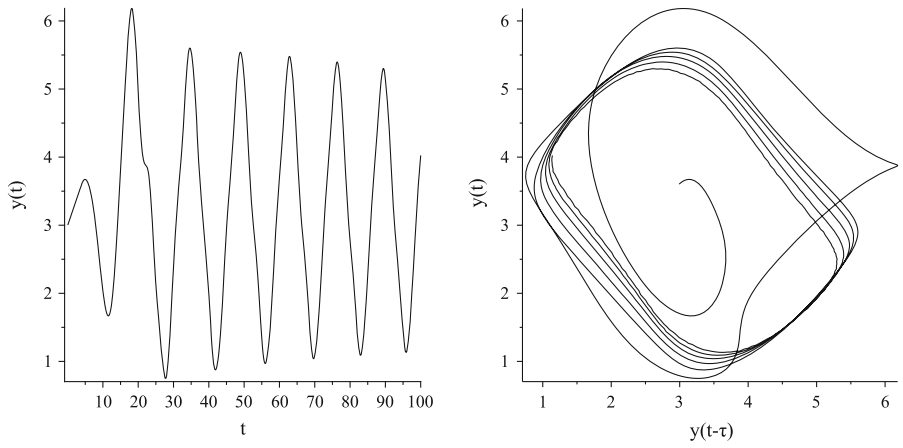


Fig. 11 Time response (left) and phase-space solution (right) for Eq. (23), with $\alpha(t) = 1 - 0.0025t$, $\lambda = 0$, $\mu = 1$, $\tau = 4$, $\varphi_0 = 2.988$ and step size $h = \frac{1}{16}$



Ultimately, replacing y_n^p in the right-hand side of (14) by (15) gives

$$\begin{aligned} y_{n+1} = & \sum_{j=0}^{\kappa-1} \phi^{(j)}(0) \frac{t_n^j}{j!} + \frac{6(\alpha_n + 1)h^{\alpha_n}}{\Gamma(\alpha_n + 4)} f(t_n, y_n^p, y_{n-m}) \\ & - \frac{2\alpha_n h^{\alpha_n}}{\Gamma(\alpha_n + 4)} f'(t_n, y_n^p, y_{n-m}) \\ & + \sum_{j=0}^{n-1} \frac{h^{\alpha_j}}{\Gamma(\alpha_j + 4)} a_{n,j} f(t_j, y_j, y_{j-m}) \\ & + \sum_{j=0}^{n-1} \frac{h^{\alpha_j+1}}{\Gamma(\alpha_j + 4)} b_{n,j} f'(t_j, y_j, y_{j-m}). \quad (19) \end{aligned}$$

4 Numerical illustrative examples

In this section, we demonstrate the efficiency and accuracy of the proposed method. For this purpose, we can analyze its accuracy and computational efficiency, in the view point of the mean absolute error (MAE) defined as

$$MAE = \frac{1}{N} \sum_{i=1}^N AE, \quad (20)$$

where $AE = |y_i^N - y_{2i}^{2N}|$, y_i^N and y_{2i}^{2N} are approximate values of $y(t)$ in t_i and N denotes the number of interior mesh points. Furthermore, we apply the measure

$$ECO = \frac{\log(MAE)}{\log(h)}, \quad (21)$$

where h denotes the uniform step size, for estimating the experimental convergence order (ECO). Note that an optimal step size can only be defined in relation to a given error tolerance. This pre-assigned value of the error, which is under the user control, will be regarded as the user-imposed tolerance. It is worth mentioning that all the numeric computations are performed by Maple v18 and the results were generated on a desktop PC with an AMD Athlon 64 X2 Dual Core Processor 5200+@2.6 GHz. For measuring the computational load, we obtain the elapsed time “E-time.” The E-time is independent of the CPU time, includes the simplification of data structures and shows the duration from when the process starts until the time it terminates with units in seconds.

4.1 Approximation of VO fractional integrals

In this subsection, the efficiency and numerical accuracy of proposed method are illustrated by two test examples. We adopt a numerical discretization formula (12) to approximate the VO fractional integral for a given functions $y(t) = t^4$ and $y(t) = t^2 \cos(t)$. Figures 1 and 3 show the VO fractional integrals of the functions $y(t) = t^4$ and $y(t) = t^2 \cos(t)$ and the magnitude of the AEs for various values of $\alpha(t)$ with uniform step size $h = 0.01$ in interval $t \in [0, 5]$. The computational results presented in Tables 1 and 2 reveal that if we increase the number of mesh points, then the MAE becomes smaller and we get a better approximation. Figures 2 and 4 show that when the time interval becomes larger, the values of MAE increase for constant step size. Therefore, to control the value of MAE, it is necessary; we reduced the step size by larger time interval. Furthermore, it is clear from Tables 1 and 2 that the proposed method has a fast convergence.

4.2 Applications

Since Mackey and Glass in 1977 [37] found chaotic behavior in a delay differential equation model of blood production in patients with leukemia, chaotic time-delay systems have been employed in numerous other practical applications in engineering, biology, economy and other disciplines [42–45].

On the other hand, delay estimation has a variety of widespread applications from satellite orbit determination to radar systems and secure communications. In addition, delay estimation has a critical role in climate prediction. A good the time-delay estimate can be a means to achieve a good model, which results in a good stability analysis [46] or control design.

In this subsection, we concentrate on the two VO fractional mathematical modeling of nonlinear dynamics, Hutchinson and Ikeda equations. The dynamical behavior of the models is studied numerically for fixed-order and VO fractional derivatives. To demonstrate the accuracy and efficiency of the proposed method, we use monotonic solutions for considered models and list results in the tables. Using a phase plane analysis, both periodic and chaotically behaving solutions are found and show the effect of VO on the dynamics behavior of the models.

Table 5 Model 2:
Comparison of MAE, for various values of $\alpha(t)$ and $\lambda = \mu = 0.4$, $\tau = 0.5$, $\varphi_0 = \frac{\pi}{2}$, $T = 25$ and different step sizes h

Step size	$\alpha(t) = 1$	$\alpha(t) = 0.95$	$\alpha(t) = 1 - 0.01t$
$h = \frac{1}{8}$	$2.345115584 \times 10^{-3}$	$3.120694402 \times 10^{-3}$	$2.499312556 \times 10^{-3}$
$h = \frac{1}{16}$	$1.220717606 \times 10^{-3}$	$1.660169046 \times 10^{-3}$	$1.321408320 \times 10^{-3}$
$h = \frac{1}{32}$	$6.222408782 \times 10^{-4}$	$8.702301770 \times 10^{-4}$	$6.816487856 \times 10^{-4}$

Table 6 Model 2:
Comparison of ECO, for various values of $\alpha(t)$ and $\lambda = \mu = 0.4$, $\tau = 0.5$, $\varphi_0 = \frac{\pi}{2}$, $T = 25$ and different step sizes h

Step size	$\alpha(t) = 1$	$\alpha(t) = 0.95$	$\alpha(t) = 1 - 0.01t$
$h = \frac{1}{8}$	2.912041752	2.774639067	2.881417652
$h = \frac{1}{16}$	2.419513698	2.308613534	2.390926987
$h = \frac{1}{32}$	2.130047841	2.033263067	2.103736758

Model 1 *The VO fractional Hutchinson equation:* Hutchinson incorporated the effect of delays into the logistic equation [47, 48]. Delays bring about interesting topological changes in the population size like damped oscillations, limit cycles and even chaos [49]. We modified the Hutchinsons equation or delay logistic equation and represent as follows:

$$\begin{cases} {}_{0+}^{V2}D_t^{\alpha(t)}y(t) = ay(t)(1 - y(t-\tau)), & 0 < \alpha(t) \leq 1, 0 < t < T \\ y(t) = 0.1, & -\tau \leq t \leq 0 \end{cases}, \quad (22)$$

where $a > 0$ is the parameter and τ is the delay time.

For comparative study, in Tables 3 and 4 the MAE and the ECO for various values of $\alpha(t)$ and different step sizes are listed. Decreasing the step size, one can obtain highly accuracy approximation solution to (22). Figure 5 shows the time history of the damped oscillatory solutions of (22) by using the proposed method for various values of $\alpha(t)$ with $a = 1.4$, $\tau = 1$ and step size $h = \frac{1}{16}$. The results show that by using the suitable VO fractional derivative functions, $\alpha(t)$, the amplitude of oscillation is reduced and damped gradually with time. In Figs. 6, 7 and 8, we depict the time responses and the phase-space solutions of the Eq. (22) with $a = 1.7$, $\tau = 1$ and step size $h = \frac{1}{16}$ for $\alpha(t) = 1$, $\alpha(t) = 0.7$ and $\alpha(t) = 1 - 0.003t$, respectively.

Model 2 *The VO fractional Ikeda equation:* The Ikeda system [50–52] was introduced to describe the dynamics of an optical bistable resonator, and the time taken for the round trip of the light across the resonator is considered as the delay time τ . The VO fractional Ikeda equation states as

$$\begin{cases} {}_{0+}^{V2}D_t^{\alpha(t)}y(t) = \mu \sin(y(t-\tau)) - \lambda y(t), & 0 < \alpha(t) \leq 1, 0 < t < T \\ y(t) = \varphi_0, & -\tau \leq t \leq 0 \end{cases}, \quad (23)$$

where $\lambda > 0$ and $\mu > 0$ are the parameters and τ is the delay time.

Physically, $y(t)$ represents the phase lag of the electric field across the resonator, μ is the light intensity injected into the system, τ is the feedback delay time in the resonator and λ is the relaxation coefficient.

We assume that $\alpha(t) = 1 - 0.0025t$ and we study the dynamic behavior of Eq. (23) in the interval $[0, 100]$. It obvious the function $\alpha(t) = 1 - 0.0025t$ is decreasing function and $\alpha(t) \in [0.75, 1]$. As shown in Figs. 9, 10 and 11, decreasing value of VO function $\alpha(t)$ from 1 to 0.75, we observe the transition from a integer-order ($\alpha(t) = 1$) behavior to a fixed-order ($\alpha(t) = 0.75$) behavior. MAE and ECO for Eq. (23) for various values of $\alpha(t)$ and different step sizes h , calculated by means of proposed algorithm using embedding delay $\tau = 4$ and embedding $\lambda = \mu = 0.4$ and $T = 25$, along with the initial condition $y(t) = \frac{\pi}{2}$ in the range $t \in (-\tau, 0)$ are summarized in Tables 5 and 6.

5 Conclusion

In this paper, a new numerical discretization formula, based on the cubic spline interpolation for approximating the VO fractional integral, is introduced and implemented. By adopting the approximation formula, we obtained a predictor–corrector method for the numerical solution of a class of nonlinear VOFDDEs. Several

illustrative VO fractional models of nonlinear dynamics are solved by new method, and the results are analyzed using phase portraits. The numerical experiments demonstrated the high accuracy and the fast convergence of the new scheme. Moreover, the results reveal that VO can act as a modulation parameter that may useful for better describing and chaos controlling of dynamic systems with time delay.

References

- Machado, J.A.T., Kiryakova, V., Mainardi, F.: Recent history of fractional calculus. *Commun. Nonlinear Sci. Numer. Simul.* **16**(3), 1140–1153 (2011). doi:[10.1016/j.cnsns.2010.05.027](https://doi.org/10.1016/j.cnsns.2010.05.027)
- Ferreira, N.M.F., Machado, J.A.T.: *Math. Methods Eng.* Springer, Netherlands (2014). doi:[10.1007/978-94-007-7183-3](https://doi.org/10.1007/978-94-007-7183-3)
- Baleanu, D., Guvenc, Z.B., Machado, J.A.T.: *New Trends in Nanotechnology and Fractional Calculus Applications*. Springer, Netherlands (2010). doi:[10.1007/978-90-481-3293-5](https://doi.org/10.1007/978-90-481-3293-5)
- Li, K., Maione, G., Fei, M., Gu, X.: Recent advances on modeling, control, and optimization for complex engineering systems. *Math. Probl. Eng.* **2015**, 1–1 (2015). doi:[10.1155/2015/746729](https://doi.org/10.1155/2015/746729)
- Oustaloup, A., Levron, F.M.B.: Frequency-band complex noninteger differentiator: characterization and synthesis. *IEEE Trans CAS-I* **47**(1), 25–39 (2000). doi:[10.1109/81.817385](https://doi.org/10.1109/81.817385)
- David, S.A., Machado, J.A.T., Quintino, D.D., Balthazar, J.M.: Partial chaos suppression in a fractional order macroeconomic model. *Math. Comput. Simul.* **122**, 55–68 (2016). doi:[10.1016/j.matcom.2015.11.004](https://doi.org/10.1016/j.matcom.2015.11.004)
- Gutiérrez-Carvajal, R.E., de Melo, L.F., Rosário, J.M., Machado, J.T.: Condition-based diagnosis of mechatronic systems using a fractional calculus approach. *Int. J. Syst. Sci.* **47**(9), 2169–2177 (2014). doi:[10.1080/00207721.2014.978833](https://doi.org/10.1080/00207721.2014.978833)
- Lopes, A.M., Machado, J.A.T.: Integer and fractional-order entropy analysis of earthquake data serie. *Nonlinear Dyn.* **84**(1), 79–90 (2016). doi:[10.1007/s11071-015-2231-x](https://doi.org/10.1007/s11071-015-2231-x)
- Coimbra, C.F.M.: Mechanics with variable-order differential operators. *Annalen der Physik* **12**(11–12), 692–703 (2003). doi:[10.1002/andp.200310032](https://doi.org/10.1002/andp.200310032)
- Diaz, G., Coimbra, C.F.M.: Nonlinear dynamics and control of a variable order oscillator with application to the van der pol equation. *Nonlinear Dyn.* **56**(1–2), 145–157 (2009). doi:[10.1007/s11071-008-9385-8](https://doi.org/10.1007/s11071-008-9385-8)
- Ramirez, L.E.S., Coimbra, C.F.M.: On the variable order dynamics of the nonlinear wake caused by a sedimenting particle. *Phys. D-Nonlinear Phenom.* **240**(13), 1111–1118 (2011). doi:[10.1016/j.physd.2011.04.001](https://doi.org/10.1016/j.physd.2011.04.001)
- Ingman, D., Suzdalnitsky, J.: Control of damping oscillations by fractional differential operator with time-dependent order. *Comput. Methods Appl. Mech. Eng.* **193**(52), 5585–5595 (2004). doi:[10.1016/j.cma.2004.06.029](https://doi.org/10.1016/j.cma.2004.06.029)
- Soon, C.M., Coimbra, C.F.M., Kobayashi, M.H.: The variable viscoelasticity oscillator. *Annalen der Physik* **14**(6), 378–389 (2005). doi:[10.1002/andp.200410140](https://doi.org/10.1002/andp.200410140)
- Ramirez, L.E.S., Coimbra, C.F.M.: A variable order constitutive relation for viscoelasticity. *Annalen der Physik* **16**(7–8), 543–552 (2007). doi:[10.1002/andp.200710246](https://doi.org/10.1002/andp.200710246)
- Sheng, Y.C.H., Sun, H., Qiu, T.: Synthesis of multifractional Gaussian noises based on variable-order fractional operators. *Signal Process.* **91**(7), 1645–1650 (2011). doi:[10.1016/j.sigpro.2011.01.010](https://doi.org/10.1016/j.sigpro.2011.01.010)
- Ostalczyk, P., Rybicki, T.: Variable-fractional-order dead-beat control of an electromagnetic servo. *J. Vib. Control* **4**(9–10), 1457–1471 (2008). doi:[10.1177/1077546307087437](https://doi.org/10.1177/1077546307087437)
- Orosco, J., Coimbra, C.F.M.: On the control and stability of variable-order mechanical systems. *Nonlinear Dyn.* **1**–16 (2016). doi:[10.1007/s11071-016-2916-9](https://doi.org/10.1007/s11071-016-2916-9)
- Samko, S.G.: Fractional integration and differentiation of variable order. *Ann. Math.* **21**(3), 213–236 (1995). doi:[10.1007/BF01911126](https://doi.org/10.1007/BF01911126)
- Lorenzo, C., Hartley, T.: Variable order and distributed order fractional operators. *Nonlinear Dynam.* **29**(1–4), 57–98 (2002). doi:[10.1023/A:1016586905654](https://doi.org/10.1023/A:1016586905654)
- Ramirez, L.E.S., Coimbra, C.F.M.: On the selection and meaning of variable order operators for dynamic modeling. *Int. J. Differ. Equ.* **2010**, 1–16 (2010). doi:[10.1155/2010/846107](https://doi.org/10.1155/2010/846107)
- Lifshits, M., Linde, W.: Fractional integration operators of variable order: continuity and compactness properties. *Mathematische Nachrichten* **287**(8–9), 980–1000 (2013). doi:[10.1002/mana.201200337](https://doi.org/10.1002/mana.201200337)
- Samko, S.G., Ross, B.: Integration and differentiation to a variable fractional order. *Integral Transforms Spec. Funct.* **1**(4), 277–300 (1993). doi:[10.1080/10652469308819027](https://doi.org/10.1080/10652469308819027)
- Samko, S.: Fractional integration and differentiation of variable order: an overview. *Nonlinear Dynam.* **71**(4), 653–662 (2013). doi:[10.1007/s11071-012-0485-0](https://doi.org/10.1007/s11071-012-0485-0)
- Sheng, H., Sun, H., Coopmans, C., Chen, Y., Bohannan, G.W.: Physical experimental study of variable-order fractional integrator and differentiator. *Eur. Phys. J. Spec. Top.* **193**(1), 93–104 (2011). doi:[10.1140/epjst/e2011-01384-4](https://doi.org/10.1140/epjst/e2011-01384-4)
- Tavares, D., Almeida, R., Torres, D.F.M.: Caputo derivatives of fractional variable order: numerical approximations. *Commun. Nonlinear Sci. Numer. Simul.* **35**, 69–87 (2016). doi:[10.1016/j.cnsns.2015.10.027](https://doi.org/10.1016/j.cnsns.2015.10.027)
- Bhrawy, A.H., Zaky, M.A.: Numerical algorithm for the variable-order caputo fractional functional differential equation. *Nonlinear Dyn.* **1**–9 (2016). doi:[10.1007/s11071-016-2797-y](https://doi.org/10.1007/s11071-016-2797-y)
- Bhrawy, A.H., Zaky, M.A.: Numerical simulation for two-dimensional variable-order fractional nonlinear cable equation. *Nonlinear Dynam.* **80**(1–2), 101–116 (2015). doi:[10.1007/s11071-014-1854-7](https://doi.org/10.1007/s11071-014-1854-7)
- Babakhani, A., Baleanu, D., Khanbabaie, R.: Hopf bifurcation for a class of fractional differential equations with delay. *Nonlinear Dynam.* **69**(3), 101–116 (2012). doi:[10.1007/s11071-011-0299-5](https://doi.org/10.1007/s11071-011-0299-5)
- Gao, Z.: A graphic stability criterion for non-commensurate fractional-order time-delay systems. *Nonlinear Dynam.* **78**(3), 2101–2111 (2014). doi:[10.1007/s11071-014-1580-1](https://doi.org/10.1007/s11071-014-1580-1)
- Moghaddam, B.P., Mostaghim, Z.S.: A novel matrix approach to fractional finite difference for solving models

- based on nonlinear fractional delay differential equations. *Ain Shams Eng. J.* **5**(2), 585–594 (2014). doi:[10.1016/j.asej.2013.11.007](https://doi.org/10.1016/j.asej.2013.11.007)
31. Moghaddam, B.P., Mostaghim, Z.S.: Modified finite difference method for solving fractional delay differential equations. *Boletim da Sociedade Paranaense de Matemtica* **35**(2), 49–58 (2016). doi:[10.5269/bspm.v35i2.25081](https://doi.org/10.5269/bspm.v35i2.25081)
 32. Ingman, D., Suzdalnitsky, J.: Application of differential operator with servo-order function in model of viscoelastic deformation process. *J. Eng. Mech.* **131**(7), 763–767 (2005). doi:[10.1061/\(ASCE\)0733-9399](https://doi.org/10.1061/(ASCE)0733-9399.0000139)
 33. Sun, H.W.H.G., Chen, W., Chen, Y.: A comparative study of constant-order and variable-order fractional models in characterizing memory property of systems, *Eur. Phys. J. Special Topics Perspectives on Fractional. Dynam. Control* **193**(185), 185–192 (2011). doi:[10.1140/epjst/e2011-01390-6](https://doi.org/10.1140/epjst/e2011-01390-6)
 34. Moghaddam, B.P., Machado, J.A.T.: A stable three-level explicit spline finite difference scheme for a class of nonlinear time variable order fractional partial differential equations. *Comput. Math. Appl.* (2016). doi:[10.1016/j.camwa.2016.07.010](https://doi.org/10.1016/j.camwa.2016.07.010)
 35. Moghaddam, B.P., Yaghoobi, S., Machado, J.A.T.: An extended predictor-corrector algorithm for variable-order fractional delay differential equations. *J. Comput. Nonlinear Dyn.* **11**(6), 061001 (2016). doi:[10.1115/1.4032574](https://doi.org/10.1115/1.4032574)
 36. Kosko, B.: Bidirectional associative memories. *IEEE Trans. Syst. Man. Cybern.* **18**(1), 49–60 (1988). doi:[10.1109/21.87054](https://doi.org/10.1109/21.87054)
 37. Mackey, M., Glass, L.: Oscillation and chaos in physiological control systems. *Science* **197**(4300), 287–289 (1977). doi:[10.1126/science.267326](https://doi.org/10.1126/science.267326)
 38. Cao, J., Lu, J.: Adaptive synchronization of neural networks with or without time-varying delay. *Chaos* **16**(1), 013133 (2006). doi:[10.1063/1.2178448](https://doi.org/10.1063/1.2178448)
 39. Sun, Z., Xu, W., Yang, X., Fang, T.: Inducing or suppressing chaos in a double-well duffing oscillator by time delay feedback. *Chaos Solitons Fractals* **27**(3), 705–714 (2006). doi:[10.1016/j.chaos.2005.04.041](https://doi.org/10.1016/j.chaos.2005.04.041)
 40. Li, L., Peng, H., Yang, Y., Wang, X.: On the chaotic synchronization of Lorenz systems with time-varying lags. *Chaos Solitons Fractals* **41**(2), 783–794 (2006). doi:[10.1016/j.chaos.2008.03.014](https://doi.org/10.1016/j.chaos.2008.03.014)
 41. Chua, L., Yang, L.I.N.: Cellular neural network: Theory. *IEEE Trans. Circuits Syst.* **35**, 1257–1272 (1988)
 42. Sun, J.: Global synchronization criteria with channel time delay for chaotic time-delay systems. *Chaos Solitons Fractals* **21**(4), 967–975 (2004). doi:[10.1016/j.chaos.2003.12.055](https://doi.org/10.1016/j.chaos.2003.12.055)
 43. Lu, H., He, Z.: Chaotic behavior in first-order autonomous continuous-time systems with delay. *IEEE Trans. Circuits Syst. I* **43**(8), 700–702 (1996). doi:[10.1109/81.526689](https://doi.org/10.1109/81.526689)
 44. Sun, J., Zhang, Y., Liu, Y., Deng, F.: Exponential stability of interval dynamical system with multidelay. *Appl. Math. Mech.* **23**(1), 95–99 (2002). doi:[10.1007/bf02437735](https://doi.org/10.1007/bf02437735)
 45. Samiei, E., Torkamani, S., Butcher, E.A.: On Lyapunov stability of scalar stochastic time-delayed systems. *Int. J. Dynam. Control* **1**(1), 64–80 (2013)
 46. Torkamani, S., Samiei, E., Bobrenkov, O., Butcher, E.A.: Numerical stability analysis of linear stochastic delay differential equations using chebyshev spectral continuous time approximation. *Int. J. Dynam. Control* **2**(2), 210–220 (2014)
 47. Hutchinson, G.E.: Circular causal systems in ecology. *Ann. N.Y. Acad. Sci.* **50**, 221–246 (1948). doi:[10.1111/j.1749-6632.1948.tb39854.x](https://doi.org/10.1111/j.1749-6632.1948.tb39854.x)
 48. Ruan, S.: Delay differential equations in single species dynamics (2006). doi:[10.1007/1-4020-3647-7-11](https://doi.org/10.1007/1-4020-3647-7-11)
 49. Strogatz, S.H., Fox, R.F.: Nonlinear dynamics and chaos: with applications to physics, biology, chemistry and engineering. *Phys. Today* **48**(3), 93 (1995). doi:[10.1063/1.2807947](https://doi.org/10.1063/1.2807947)
 50. Ikeda, K., Daido, H., Akimoto, O.: Optical turbulence: Chaotic behavior of transmitted light from a ring cavity. *Phys. Rev. Lett.* **45**(9), 709–712 (1980). doi:[10.1103/PhysRevLett.45.709](https://doi.org/10.1103/PhysRevLett.45.709)
 51. Ikeda, K., Matsumoto, M.: Study of a high-dimensional chaotic attractor. *J. Stat. Phys.* **44**(5–6), 955–983 (1986). doi:[10.1007/BF01011917](https://doi.org/10.1007/BF01011917)
 52. Ikeda, K., Matsumoto, M.: High-dimensional chaotic behavior in systems with time-delayed feedback. *Physica D* **29**(1–2), 223–235 (1987). doi:[10.1016/0167-2789\(87\)90058-3](https://doi.org/10.1016/0167-2789(87)90058-3)